Heliyon 9 (2023) e21463

Contents lists available at ScienceDirect

Heliyon

journal homepage: www.cell.com/heliyon

Integrated microbiome and metabolome analysis reveals a distinct microbial and metabolic signature in Graves' disease and hypothyroidism

Wen Jiang [a,1], Ganghua Lu [a,1], Tingting Qiao [a], Xiaqing Yu [a], Qiong Luo [a], Junyu Tong [a], Suyun Fan [a], Li Chai [a], Dingwei Gao [a], Ru Wang [a], Chengwen Deng [a], Zhongwei Lv [a,**], Dan Li [b,*]

[a] Department of Nuclear Medicine, Shanghai Tenth People's Hospital, Tongji University School of Medicine, Shanghai, China
[b] Department of Nuclear Medicine, Sun Yat-sen Memorial Hospital, Sun Yat-sen University, Guangzhou, China

ARTICLE INFO

Keywords:
Graves' disease
Clinical hypothyroidism
Microbiota
16S rRNA gene sequencing
Non-targeted metabolomics

ABSTRACT

Recent studies reveal that imbalanced microbiota is related to thyroid diseases. However, studies on the alterations in fecal metabolites in Graves' disease and clinical hypothyroidism patients are insufficient. Here, we identified 21 genera and 53 metabolites that were statistically significant among Graves' disease patients, hypothyroidism patients, and controls integrating microbiome and untargeted metabolome analysis. Disease groups revealed a decreased abundance in butyrate-producing microbiota and an increased abundance in potentially pathogenic microbiota. Lipids molecules were the major differential metabolites identified in all fecal samples. Network analysis recognized that microbiota may affect thyroid function by targeting specific metabolites. We further identified specific microbiota and metabolites that could distinguish Graves' disease patients, hypothyroidism patients, and controls. Our study reveals a distinct microbial and metabolic signature in hypothyroidism patients and Graves' disease patients and further validates the potential role of microbiota in thyroid diseases, providing new ideas for future research into the etiology and clinical intervention of thyroid diseases.

1. Introduction

The thyroid, the largest endocrine gland in adults, regulates growth and development, energy, glucose, lipid metabolism, and thermogenesis via thyroid hormone synthesis, affecting the functions of almost all organs [1,2]. Changes in circulating thyroid hormone levels can cause thyroid dysfunction, manifesting as hyperthyroidism or hypothyroidism [3]. Graves' disease (GD), the most common cause of hyperthyroidism, can cause certain hypermetabolic symptoms, including tachycardia, sweating, heat intolerance, and even worse, cardiac arrhythmias and atrial fibrillation [4]. Congenital thyroid function deficiencies, thyroidectomy, and radioiodine treatment are common causes of hypothyroidism (HT) [5]. Thyroid dysfunction significantly impacts their physiological functioning and has a serious negative impact on patients' quality of life. Nevertheless, a significant gap remains in understanding the

* Corresponding author.
** Corresponding author.
E-mail addresses: Lvzwjs2020@163.com (Z. Lv), plumredlinda@163.com (D. Li).
[1] These authors contributed equally to this work.

https://doi.org/10.1016/j.heliyon.2023.e21463
Received 13 January 2023; Received in revised form 11 October 2023; Accepted 21 October 2023
Available online 3 November 2023

specific pathogenesis of GD and HT, and further research is necessary to identify a theoretical basis for the prevention and prognosis of thyroid disorders.

Accumulating studies have demonstrated intestinal microbial alterations might be related to thyroid diseases [6–8]. Prior studies have also reported that patients with GD and Hashimoto's thyroiditis exhibit a disruption in their intestinal microbiomes, suggesting that gut microbiota may play a vital role in the pathogenesis of thyroid diseases [9,10]. A study has reported that the pathological changes and the increased permeability of the intestinal mucosa lead to the leakage of intestinal microbiota and metabolites into the bloodstream, leading to a continuous inflammatory stimulus, ultimately, autoimmune disease [11,12]. These findings suggest a potential relationship between intestinal microbiota and the thyroid.

Although associations between thyroid diseases and gut microbiota have previously been reported, studies on fecal metabolite alterations among GD and HT patients are insufficient. Multi-omics analysis was integrated to identify specific intestinal microbiota and metabolites that may mediate thyroid-intestine interactions. Moreover, previous studies offer limited information regarding the relationship between gut microbiota and thyroid function disorders but rare secondary validation. Thus, we validated the causal role of gut microbiota in thyroid disorders by transplanting fecal microbiota from GD and HT patients into antibiotic-treated mice. We aim to bridge the research gaps in the gut-thyroid axis, providing new insights into the pathophysiology and novel diagnostic strategies for thyroid diseases.

2. Materials and methods

2.1. Recruitment of participants

Subjects were initially diagnosed patients recruited from the Department of Nuclear Medicine, Shanghai Tenth People's Hospital, between June 2020 and June 2021. The inclusion criteria for GD patients were as follows: 1) elevated thyroid hormone and decreased serum thyroid stimulating hormone (TSH) levels; 2) diffuse goiter and increased thyroid vascularity on ultrasonography; and 3) positive serum thyroid stimulating hormone receptor antibody (TRAb) [13]. Inclusion criteria for HT patients included decreased serum free thyroxine (FT4) and increased TSH [5]. The inclusion of controls was based on normal thyroid ultrasound and clinical indicators of thyroid function. Exclusion criteria for all subjects included: 1) malignancy; 2) other gastrointestinal and metabolic diseases (inflammatory bowel disease and type 2 diabetes); 3) history of abdominal surgery that may interfere with the microbiome; 4) patients receiving parenteral nutrition; 5) exposure to any anti-tumor therapy or radiation within one month before stool sampling; 6) use of any antibiotics, probiotics, prebiotics, steroids, or immune-suppressants within one month before stool sampling; and 7) unhealthy lifestyle (smoking and alcohol consumption).

Finally, 117 untreated patients, including 39 GD patients (12 males, 27 females, age 16–65) and 78 HT patients (34 males, 44 females, age 16–73), were enrolled in this study. Simultaneously, 48 healthy controls matched for age, gender, and body mass index (BMI) (18 males, 30 females, age 22–71) were recruited from the physical examination center. All study subjects were Han nationality and lived in the eastern coastal provinces of China with a balanced diet. Demographic information and clinical examination data from all participants were collected at enrollment. This study was approved by the Ethics Committee of Shanghai Tenth People's Hospital (ethics number 2020-KN73-01) and conducted under the guidance of the World Medical Association and the Declaration of Helsinki. In addition, all research subjects were informed of the purpose of the study at the time of recruitment and voluntarily provided written informed consent to publish the study data.

2.2. Sample collection, thyroid function, and autoantibody tests

Fecal samples of participants who fasted overnight ($\geq$8 h) were collected, quenched with liquid nitrogen, and stored at $-80\,^{\circ}C$ until microbial DNA and metabolite extraction. Peripheral blood (6 mL) was collected from all participants and stored at 4 °C for routine thyroid function and autoantibody tests. Serum levels of free triiodothyronine (FT3), FT4, total triiodothyronine (TT3), total thyroxine (TT4), TSH, and TRAb were measured using a chemiluminescent immunoassay (Beckman Coulter, Fullerton, CA, USA). The reference ranges were defined as follows: FT3 2.80–6.30 pmol/L; FT4 10.50–24.40 pmol/L; TT3 1–3 nmol/L; TT4 55.50–161.30 nmol/L; TSH 0.38–4.34 mIU/L; and TRAb 0.00–1.75 IU/L.

2.3. DNA extraction, polymerase chain reaction amplification, and Miseq sequencing

The E.Z.N.A. ® soil DNA kit (Omega Bio-tek, Norcross, GA) was used to extract bacterial DNA from fecal samples. The bacterial DNA concentration was determined using Nanodrop 2000 (Thermo Scientific, Wilmington, USA). The extracted DNA was stored at $-20\,^{\circ}C$ to prevent degradation. Specific primers 338F (5′-ACTCCTACGGGAGGCAGCAG-3′) and 806R (GGACTACHVGGGTWTCTAAT-3′) targeting V3–V4 variable region were used to complete polymerase chain reaction amplification, and testing on each sample was repeated three times to ensure the reliability of subsequent microbial and metabolic analysis [14]. The AxyPrep DNA Extraction Kit (Axygen Biosciences, USA) was used to purify the amplicons, and QuantiFluorTM-ST (Promega, USA) was used for quantitative analysis. Afterward, the purified amplicons were pooled in equimolar concentrations, and paired-end sequencing analysis was performed using the Illumina Miseq PE300 platform (Illumina Sandiego, USA).

2.4. Fecal metabolite extraction

Briefly, 400 μL methanol: water (4:1, v/v) solution was mixed with a 50 mg fecal sample. The sample was placed in the high-throughput tissue crusher Wonbio-96c (Shanghai Wanbo Biotechnology Co., Ltd., China) for 6 min at 50 Hz. Then, the mixture was vortexed for 30 s and sonicated at 40 kHz for 30 min at 5 °C. Subsequently, the mixture was incubated at −20 °C for 30 min to precipitate proteins. After centrifugation at 13000×*g* for 15 min at 4 °C, the supernatant was transferred to a sample bottle for liquid chromatography-mass spectrometry (LC-MS) analysis in the positive and negative ion modes. Meanwhile, 10 μL of supernatant from each sample was mixed for quality control (QC). This was injected at regular intervals (every eight samples) to monitor the stability of the analysis.

2.5. Microbial analysis of 16S rRNA gene sequencing

According to the overlap relationship, the paired-end reads obtained from the Illumina Miseq PE300 high-throughput sequencing were spliced into a target sequence and filtered for QC. The chimera was eliminated using UCHIME software (version 4.2.40) to optimize sequence [15]. The Ribosomal Database Project Classifier (version 2.11, http://sourceforge.net/projects/rdp-classifier/) was applied to perform species classification annotations on the optimal sequences according to the Silva database (Release128, https://www.arb-silva.de/documentation/release-128/) with a confidence threshold of 70 %. Operational taxonomy units (OTUs) were clustered with a 97 % similarity cut-off by UPARSE software (version 7.1, http://drive5.com/uparse/). OTUs accounting for less than 0.005 % of the total sequences were removed to eliminate such presumed spurious sequences [16].

2.6. Data preprocessing of LC-MS

The LC-MS raw data were imported into progenesis QI 2.3 (Nonlinear Dynamics, Waters, USA) for peak detection and comparison. Subsequently, a data matrix composed of retention time, mass-to-charge ratio values, and peak intensity was generated. The qualitative and quantitative results regarding specific metabolites were obtained. Metabolic datasets were required to be preprocessed before multivariate statistical analysis. The pre-processing methods were as follows: 1) data filtering included the removal of samples with >50 % missing values; 2) simulated filling of missing values according to one-half of the minimum metabolite value and normalization of the total peaks; and 3) elimination of QC samples with a relative standard deviation > 30 %. Finally, after logarithmic transformation, the pre-processed datasets were prepared for further analysis.

2.7. Multivariate statistical analysis

Our data were processed using IBM SPSS (Version 20.0) and R package (Version 3.4.3). The clinical characteristics of the subjects were expressed as the mean ± standard deviation, and *P*-values were determined using the Kruskal-Wallis test. The intestinal microbiota abundances and alpha diversities were analyzed using the Chao and Shannon indices. Partial Least Squares Discriminant Analysis (PLS-DA) was used to evaluate for differences in the distribution of microbial communities across the three groups. The beta diversities and statistical significances were determined between the groups using (Permutational Multivariate Analysis of Variance (PERMANOVA). Pairwise comparisons using the Mann-Whitney *U* test and linear discriminant analysis (LDA) effect size (LEfSe) analysis were used at the phylum and genus levels to investigate the differential microbiota among the three groups [14]. The differences were considered statistically significant when the average abundance level of the gut microbiota reached >0.1 %, LDA value > 3, and $P < 0.05$.

SIMCA software (Version 16.0.2, Sartorius Stedim Data Analytics AB, Umea, Sweden) was used to perform multivariate statistical analysis between the GD, HT, and control groups. The Orthogonal projections to latent structures-discriminant analysis (OPLS-DA) modeling were used to identify the distribution characteristics of metabolites across the three groups. Then, the corresponding

Table 1
Baseline characteristics and clinical markers of all participants.

Parameters	GD group (n = 39)	HT group (n = 78)	Control group (n = 48)	*P* value
Demographics				
Age (years)	39.51 ± 12.41	45.26 ± 14.30	41.67 ± 14.62	0.117
Gender (Male/Female)	12/27	34/44	18/30	0.399
BMI (kg/m^2)	21.98 ± 0.48	22.36 ± 1.55	22.21 ± 1.67	0.138
Thyroid biochemical markers				
FT3 (pmol/L)	19.69 ± 9.28	1.44 ± 0.65	3.61 ± 0.49	<0.001***
FT4 (pmol/L)	49.96 ± 26.03	3.92 ± 1.49	12.94 ± 1.28	<0.001***
TT3 (nmol/L)	6.10 ± 3.03	0.53 ± 0.24	1.85 ± 0.48	<0.001***
TT4 (pmol/L)	237.34 ± 88.55	19.38 ± 13.33	79.00 ± 12.21	<0.001***
TSH (mIU/L)	0.11 ± 0.33	118.05 ± 36.60	2.22 ± 1.02	<0.001***
TRAB (IU/L)	17.51 ± 14.49	0.72 ± 1.15	2.46 ± 1.27	<0.001***

Note: All data, except gender, are shown as the mean ± standard deviation. HT, hypothyroidism; GD, Graves' disease; BMI: body mass index; FT3: free triiodothyronine; FT4: free thyroxine; TT3: total triiodothyronine; TT4: total thyroxine; TSH: thyroid-stimulating hormone; TRAB: thyroid stimulating hormone receptor antibody. ***$P < 0.001$.

permutation test was used to obtain R2 and Q2 values to validate each OPLS-DA model's reliability and avoid overfitting. Corresponding variable importance in the projection (VIP) values, reflective of the contribution to the distribution between groups, were generated using the OPLS-DA models. Differential metabolites were mapped to their biochemical pathways based on the Kyoto

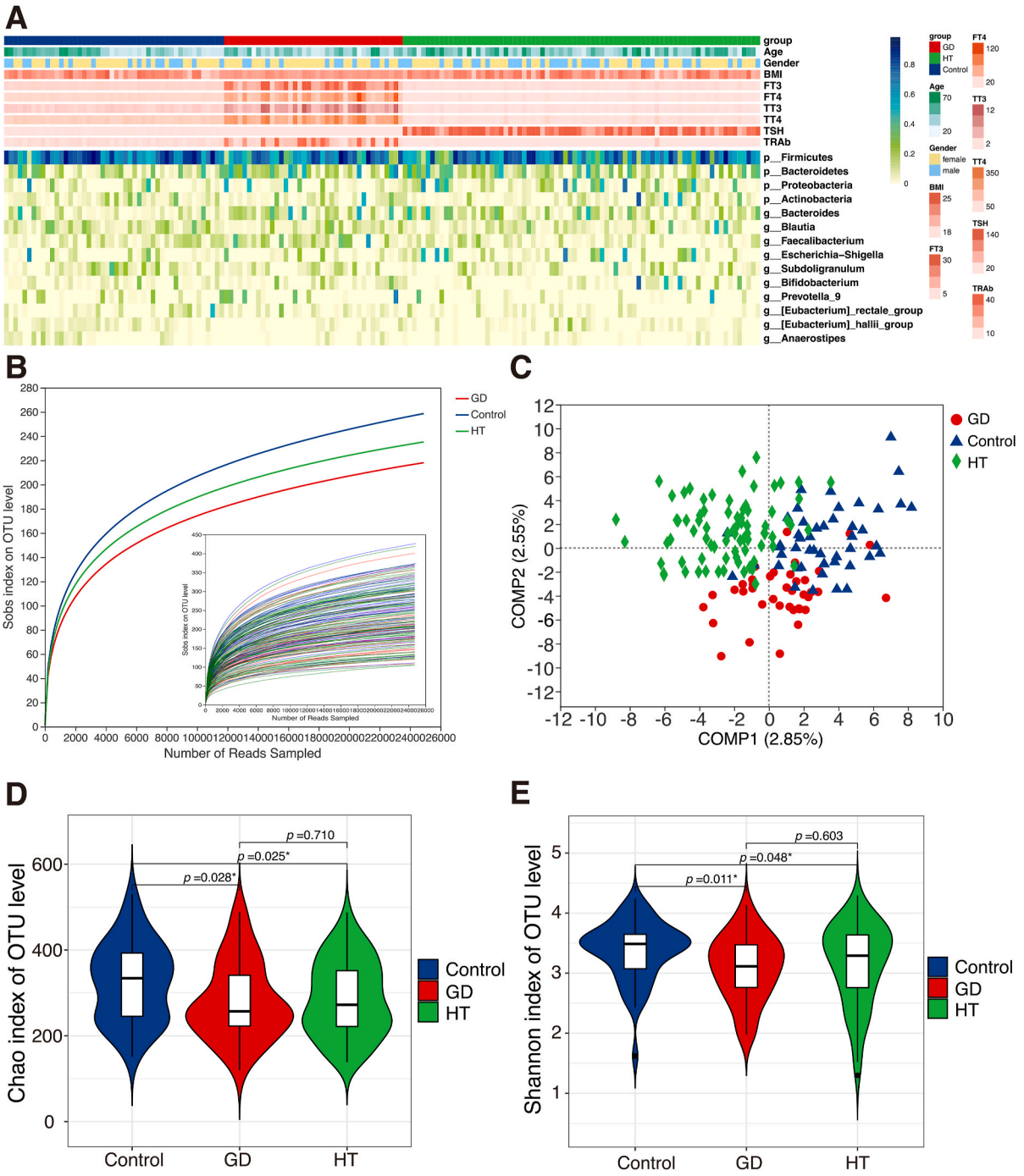

Fig. 1. Intestinal microbial diversities in the HT, GD, and control groups. (**A**) The demographic information, thyroid biochemical markers, and the abundances of the dominant phyla and genera (top 10) from the 165 participants; (**B**) Rarefaction curves (Sobs index) for the HT, GD, and control groups at the OTU level; (**C**) Differences in microbial composition (beta diversity) between the GD, HT, and control groups based on the PLS-DA model; (**D, E**) Comparisons of the mean relative abundances (Chao index) and alpha diversity (Shannon index) of gut microbiota between the GD, HT, and control groups at the OTU level. HT, hypothyroidism; GD, Graves' disease; FT3: free triiodothyronine; FT4: free thyroxine; TT3: total triiodothyronine; TT4: total thyroxine; TSH: thyroid-stimulating hormone; TRAB: thyroid stimulating hormone receptor antibody; OTU, operational taxonomic unit; PLS-DA, Partial Least Squares Discriminant Analysis; $^{*}P < 0.05$.

Encyclopedia of Genes and Genomes (KEGG) database using MetboAnalyst 5.0 (http://www.metaboanalyst.ca/) [17]. Superclass refers to the classification of metabolites as matched in the Human Metabolome Database. Spearman correlation coefficients were generated to characterize the correlations between microbiota, metabolites, and clinical indicators. The interaction network plots were visualized using Cytoscape (Version 3.7.1) [18]. The metabolites were considered to differ significantly between groups when VIP value > 1 and $P < 0.05$.

3. Results

3.1. Study population

Stool samples for multi-omics sequencing were derived from 78 HT, 39 GD, and 49 healthy controls. Table 1 summarizes the baseline information and thyroid biochemical indicators of the 165 participants. Age, gender, and BMI did not differ significantly between the HT, GD, and control groups. Fig. 1A illustrates an overview of the clinical traits of all participants.

3.2. Landscape of the gut microbiota in HT, GD, and control groups

This study generated 8,224,714 high-quality sequences from the 165 fecal samples using Illumina MiSeq high-throughput sequencing. This included 17 phyla, 323 genera, and 1320 OTUs. The rarefaction curves (Sobs index) gradually flattened as the number of sequences increased, indicating that the sequencing data was sufficient to reflect the microbial profiles of the subjects (Fig. 1B). Additionally, the rarefaction curves of the HT and GD groups were lower than those of the controls, suggesting a decrease in the number of species detected in patients. PLS-DA plot demonstrated that gut microbiota tends to cluster by group, reflecting the significant distinction in microbial composition among the three groups (PERMANOVA, $R^2 = 0.037$, $P = 0.001$, Fig. 1C). The Chao and Shannon indices, indicating the microbial alpha richness and diversity, were analyzed at the OTU level (Table S1). The Chao index was

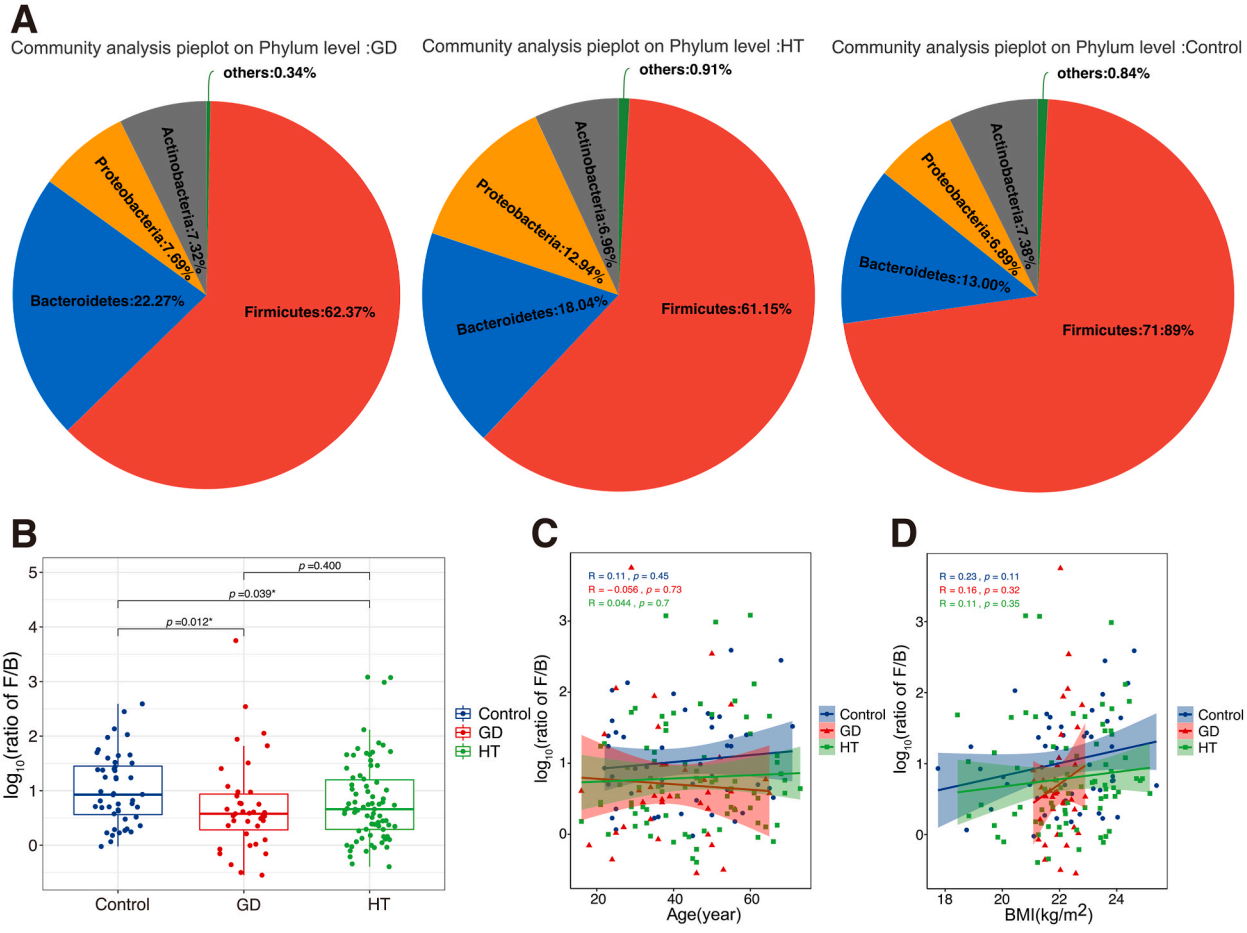

Fig. 2. Microbial composition in the HT, GD, and control groups at the phylum and genus levels. (**A**) The composition ratios of the dominant phyla in the HT, GD, and control groups; (**B**) Statistical analysis of the F/B ratio for each group; (**C, D**) Correlations between F/B ratio and age or BMI in the GD, HT, and control groups. HT, hypothyroidism; GD, Graves' disease; F/B, *Firmicutes* to *Bacteroidetes*; BMI, body mass index; $*P < 0.05$.

significantly lower in both the HT and GD groups than in controls ($P = 0.025$, 0.028, respectively), with the GD index slightly lower than the HT group ($P = 0.710$, Fig. 1D). Similarly, the Shannon index of the HT and GD groups was lower than that of the controls ($P = 0.048$, 0.011, respectively), with the HT group having a slightly higher Shannon index than the GD group ($P = 0.603$, Fig. 1E).

The pie charts visually demonstrate that *Firmicutes, Bacteroidetes, Proteobacteria,* and *Actinobacteria* are the dominant phyla in three groups, though in different proportions (Fig. 2A). Fig. 1A depicts the distribution of the dominant phyla and genera richness in each sample. *Firmicutes* was the most abundant phylum in almost all samples. Given that abnormal ratios of *Firmicutes* to *Bacteroidetes* (F/B) are related to many diseases, we also investigated variations in the F/B ratios between the three groups [19,20]. The F/B ratio was significantly lower in the HT and GD groups than in the controls ($P = 0.039$, 0.012, respectively, Fig. 2B), with a slight increase F/B ratio in the HT group than in the GD group. It has been widely reported that the F/B ratio may be influenced by age and BMI; therefore, we also examined the association between the F/B ratio and age and BMI [21,22]. However, our samples did not find a significant relationship between the F/B ratio and either age or BMI (Fig. 2C and D).

3.3. Species analysis in the HT, GD, and control groups

Statistical significances of microbiota were determined by pairwise comparison (HT versus Control, GD versus Control, and HT versus GD) using the Mann-Whitney *U* test and LEfSe analysis, respectively. Our study identified microbiota that differed between the HT, GD, and control groups only if both tests indicated statistical significance. Finally, we identified 29 genera that differed among all groups (LDA value > 3, $P < 0.05$, Table S2). Considering that eight genera were not found in significant numbers (relative abundances <0.1 %), they were eliminated from the next analysis, leaving the top 21 genera. Fig. 3 displays the top 10 genera screened for significance using the Mann-Whitney *U* test for each pairwise comparison, while Fig. S1 indicates all genera with LDA value > 3 and $P < 0.05$ as determined by the LEfSe analysis. The proportions of the top 10 differential genera were significantly lower in HT patients than in the controls, except for *Bacteroides*, which was significantly higher ($P < 0.05$, Fig. 3). The proportions of *Bacteroides* and *Lactobacillus* were significantly increased in GD patients than in the controls, while the proportions of *Blautia, [Eubacterium]_hallii_group*, and *Collinsella* were significantly decreased ($P < 0.05$, Fig. 3). Additionally, *Faecalibacterium, Hungatella*, and *unclassified_f_Lachnospiraceae* were significantly enriched in GD patients than in HT patients, while *unclassified_f_Peptostreptococcaceae,* and *Clostridium_sensu_stricto_1* were significantly decreased ($P < 0.05$, Fig. 3). The LEfSe results were similar to the Mann-Whitney *U* test at the genus level (LDA value > 3, $P < 0.05$, Fig. S1).

3.4. Metabolic profiling in the HT, GD, and control groups

We successfully quantified the 339 metabolite levels using non-target liquid LC-MS metabolomics. The OPLS-DA, with better validity and resolving power, revealed that certain metabolites could distinguish HT, GD, and controls during pairwise comparisons (Fig. 4A, S2A–B). Then, we used the permutation test to verify the validity of the OPLS-DA model. The Q2 regression line intercepted

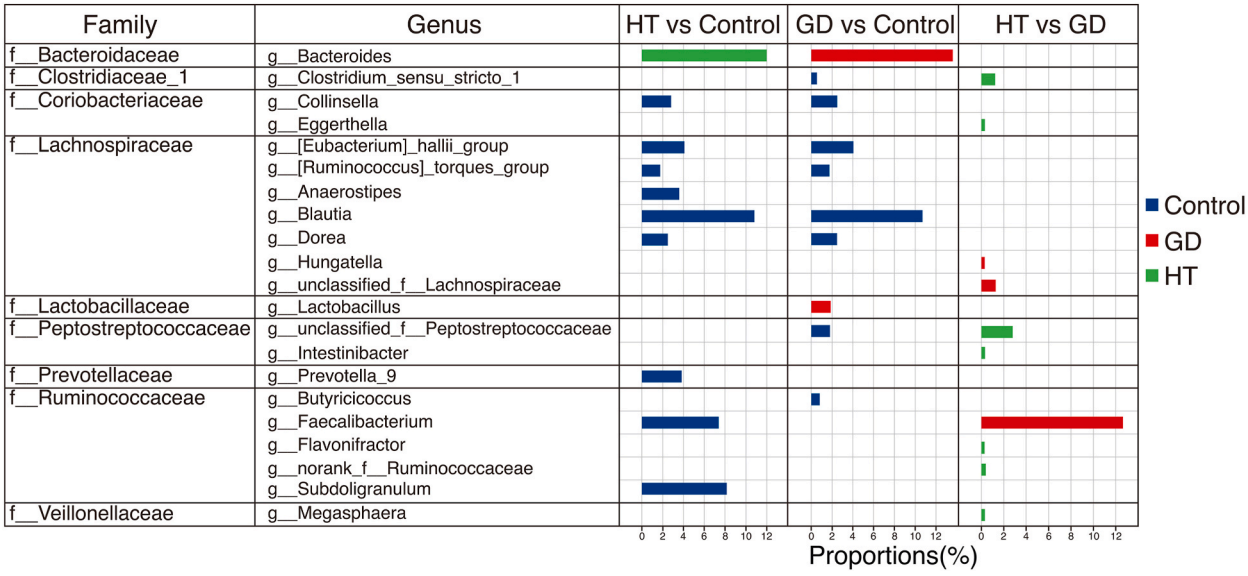

Fig. 3. Mann-Whitney *U* test plots of the pairwise comparisons between the HT, GD, and control groups. This figure presents the top 10 genera that differed between groups in each pairwise comparison (HT versus Control, GD versus Control, and HT versus GD) according to the Mann-Whitney *U* test. The family and genus levels are sorted alphabetically. Bar size corresponds to the proportion of gut microbiota, and the color represents the group with elevated levels. Green represents the HT group, red represents the GD group, and blue represents the control group. HT, hypothyroidism; GD, Graves' disease.

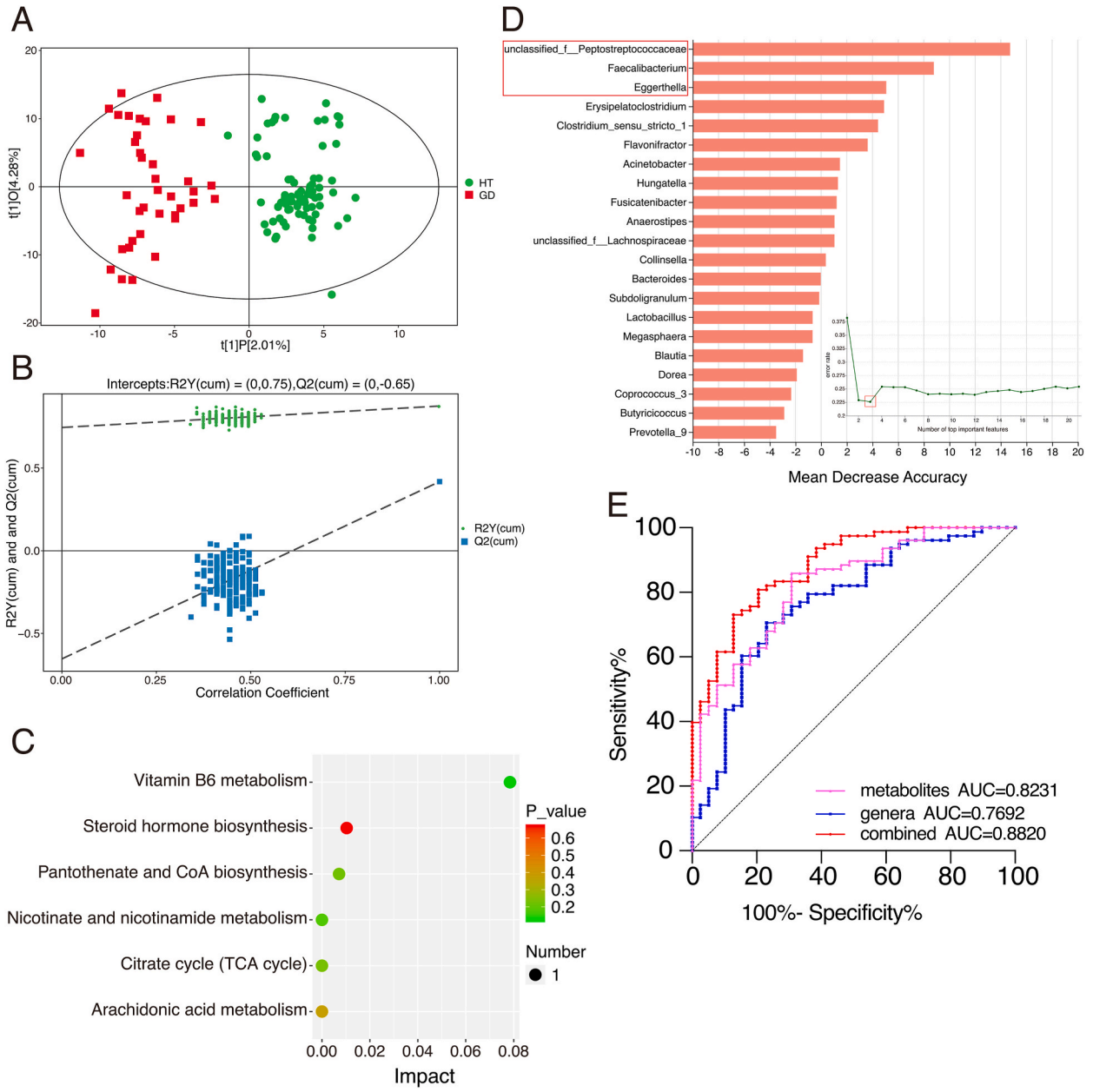

Fig. 4. Metabolic traits across the HT and GD. (**A**) OPLS-DA score plot between the HT and GD groups (R2X = 0.0629, R2Y = 0.875, Q2 = 0.418); (**B**) Permutation test for the OPLS-DA model (R2Y = 0.959, Q2 = −0.65); (**C**) KEGG functional pathways (level 3) annotated for all of the differential metabolites; (**D**) Random forest analysis of the 21 microbiota between the HT and GD groups based on 10-fold cross-validation; (**E**) ROC curves generated from the top three genera with the lowest error rates, the eight metabolites with VIP >2, and a combination of the three genera and eight metabolites to distinguish HT from GD. HT, hypothyroidism; GD, Graves' disease; OPLS-DA, orthogonal projections to latent structures-discriminant analysis; VIP, variable importance in projection; ROC, receiver operating characteristic curve; AUC, the area under the curve.

the Y axis negatively, indicating that the OPLS-DA model was adequate to determine differences between the HT and GD groups (R2Y = 0.959, Q2 = −0.65, Fig. 4B). The validity of the other two pairwise comparisons (HT versus Controls and GD versus Controls) were verified similarly (Figs. S2C–D).

Subsequently, various metabolites with VIP value > 1 and $P < 0.05$ were investigated using stratified analysis. Twenty-nine metabolites significantly differed between HT and GD patients (Fig. 5, Table S3). Twenty metabolites significantly differed between GD patients and controls, whereas 27 metabolites significantly differed between HT patients and controls (Fig. 5, Tables S4–S5). Next, we performed KEGG functional annotation to determine the roles of these differential metabolites using MetboAnalyst 5.0. Fig. 4C illustrates the KEGG pathways at level 3 for all differential metabolites. Specifically, 5,6-DHET was involved in Arachidonic acid

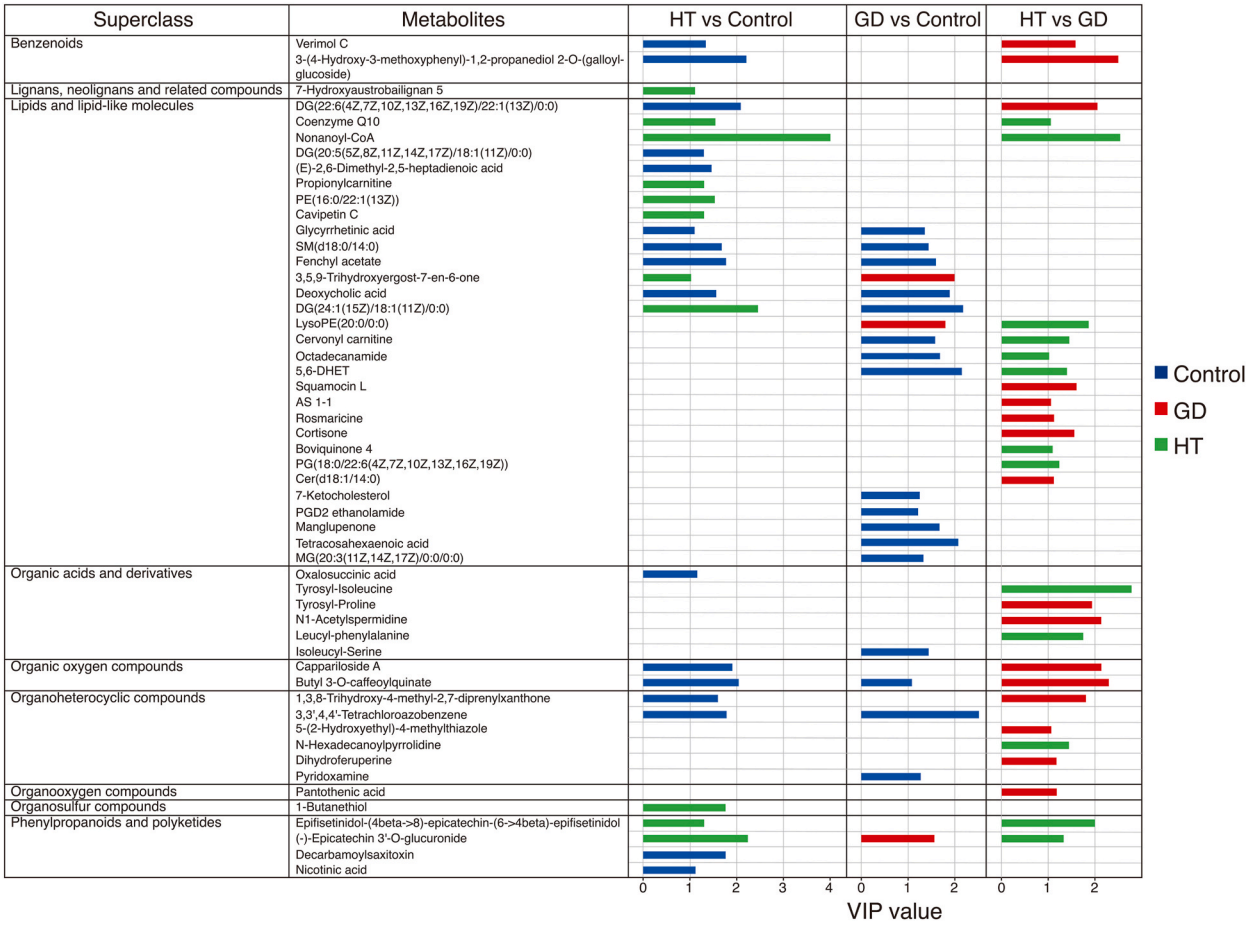

Fig. 5. VIP values for the differential metabolites in each pairwise comparison. This figure illustrates all differential metabolites with VIP value > 1 and $P < 0.05$ for each pairwise comparison (HT versus Control, GD versus Control, and HT versus GD). Superclass refers to the metabolite classification as matched in the Human Metabolome Database, and these are sorted alphabetically. Bar size corresponds to the VIP value, and the color represents the group with elevated metabolite. Green represents the HT group, red represents the GD group, and blue represents the control group. HT, hypothyroidism; GD, Graves' disease, VIP, variable importance in projection.

metabolism, and cortisone was involved in Steroid hormone biosynthesis, both lipid metabolisms. The Citrate cycle (TCA cycle) involved oxalosuccinic acid. Pyridoxamine, nicotinic acid, and pantothenic acid were involved in vitamin B6 metabolism, nicotinate and nicotinamide metabolism, and pantothenate and CoA biosynthesis, respectively, cofactors and vitamin metabolism.

3.5. Network analysis among the microbiota, metabolites, and thyroid hormones

Subsequently, we performed the co-occurrence analysis to investigate the relationships among the differential microbiota, metabolites, and thyroid clinic indicators. Some butyrate-producing bacteria, such as *Blautia* and *unclassified_f_Lachnospiraceae*, were only linked to metabolites, while other potentially pathogenic bacteria that were significantly increased in patients (*Flavonifractor* and *Bacteroides*) were directly related to thyroid hormones besides being closely related to metabolites (Fig. 6). We artificially divided the metabolites into three clusters: cluster 1, containing metabolites only associated with thyroid function, cluster 2, containing lipids that served as a communication link between thyroid function and microbiota; and cluster 3, containing metabolites only associated with gut microbiota.

3.6. Random forest (RF) analysis

We compared receiver operating characteristic curves (ROC) generated from genera with the lowest prediction error rates, significant metabolites (VIP value > 2), and a combination of both using RF analysis to examine whether certain microbiota and metabolites can characterize the gut microbiota changes of patients with thyroid function disorders. RF analysis using the 10-fold cross-validation method revealed the highest accuracy when the top three genera (*unclassified_f_Peptostreptococcaceae*, *Faecalibaterium*, and *Eggerthella*) were used to distinguish HT from GD, yielding an area under the curve (AUC) of 0.7692 (95 % confidence interval (CI) =

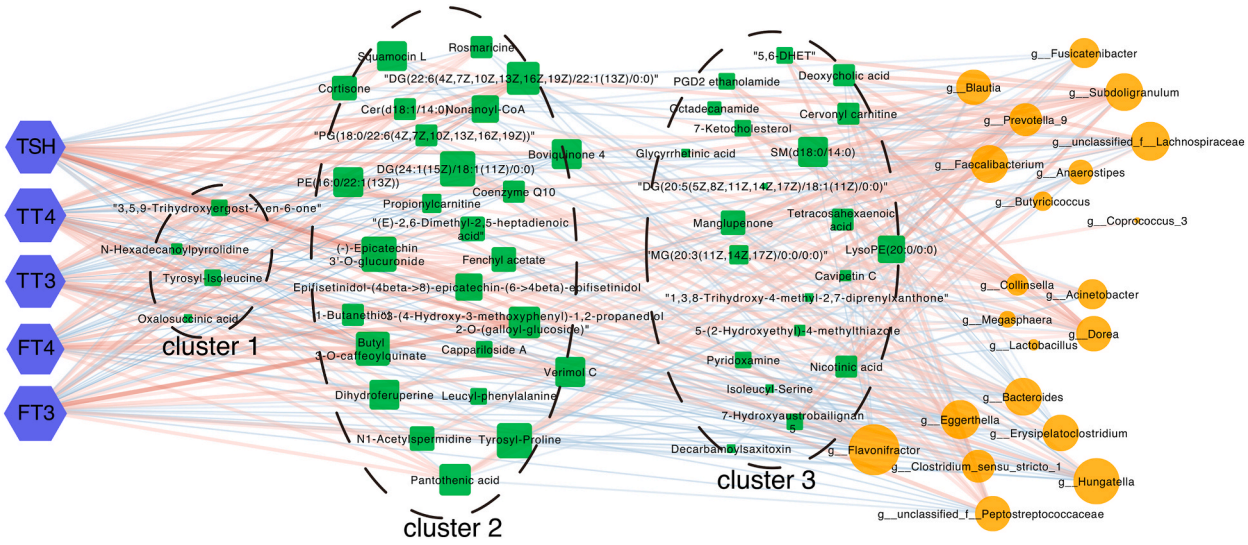

Fig. 6. A network analysis of all differential microbiota, fecal metabolites, and thyroid clinical indicators across the HT, GD, and control groups. In the network, Spearman correlation coefficient values below −0.1 (negative correlation) were indicated as blue edges, and coefficient values above 0.1 (positive correlation) were indicated as red edges. Metabolites were artificially divided into three clusters: cluster 1 was associated with gut microbiota, cluster 2 was primarily composed of lipids having complex correlations with the thyroid and microbiota, and cluster 3 was associated with the thyroid. The size of the nodes represents the degree of connectivity. Edge thickness indicates the range of correlation coefficient values. The pentagons are thyroid clinical indicators, the squares are metabolites, and the circles are microbiota.

0.6763–0.8622, Fig. 4D and E). Similarly, we selected eight metabolites with VIP value > 2 that differed significantly between the HT and GD groups for ROC, generating an AUC of 0.8231 (95 % CI = 0.7433–0.9010, Fig. 4E). Notably, AUC was significantly increased to 0.8820 (95 % CI = 0.8199–0.9441) by combining the three genera with the eight metabolites, suggesting that microbiota in combination with metabolites has a better performance to discriminate HT from GD (Fig. 4E). Furthermore, the combination of intestinal microbiota and metabolites may improve the ability to distinguish HT or GD patients from controls, with AUCs of 0.9912 (95 % CI = 0.9765–1.000) and 0.9802 (95 % CI = 0.9568–1.000), respectively (Fig. S3).

4. Discussion

Decreased alpha diversity of gut microbiota was observed in HT and GD patients, consistent with previous findings regarding GD and primary hypothyroidism patients [9,23]. The F/B ratio in the HT group overall was not elevated as it was in obese patients [19]. We speculate that the proportions of *Firmicutes* and *Bacteroidetes* may be indirectly regulated by thyroid hormones, with microbial interactions also likely contributing to the reduced F/B ratio. The correlations between microbiota and thyroid hormones provide a theoretical basis for these assumptions. A further metagenomic investigation would be necessary to elucidate these additional factors more precisely.

Twenty-one genera whose abundances significantly differed among the HT, GD, and control groups were identified (relative abundance >0.01 %, LDA value > 3, and $p < 0.05$). The butyrate-producing microbiota, including *Blautia, Subdoligranulum, Anaerostipes, unclassified_f_Lachnospiraceae, Fusicatenibacter, Butyricicoccus,* and *Coprococcus_3*, in HT and GD patients were significantly decreased compared to controls, consistent with previous studies presenting drops in these microbiota in other diseases [24–26]. Butyrate plays an anti-inflammatory role by reinforcing the intestinal mucosal barrier and maintaining intestinal epithelium integrity [27]. Nagendra Singh et al. discovered that butyrate exerted anti-inflammatory and anti-carcinogenic effects in the colon by activating G-protein coupled receptor 109a signaling, promoting regulatory T cells and interleukin-10 production, inducing T cell proliferation, and increasing interleukin-18 secretion [28]. Considering the intimate associations of T cells in thyroid diseases, we hypothesized that butyrate may also indirectly regulate thyroid function by affecting intestinal mucosal permeability and T cell differentiation. More precise targeted assays for short-chain fatty acids, especially butyrate, are required to obtain a comprehensive view of this relationship because no data on intestinal butyrate changes in our patients were available during fecal metabolomics.

Furthermore, the increased potentially pathogenic microbiota may promote thyroid hormone disorders. *Bacteroides*, the most abundant genus in the HT and GD groups, may play a dominant pathogenic role in the disease progression. *Bacteroides* impair the intestinal mucosal barrier by reducing mucin synthesis and allowing toxins and bacterial metabolites to leak into the bloodstream, activating inflammatory responses [29]. The increased abundance of *Lactobacillus* in thyroid patients also attracted our attention, consistent with findings in autoimmune hepatitis [30]. It is thought that this result may be related to the immune response activated by the microbiota through cross-antigenic reactions [31].

However, the influences of other pathogenic microbiota in the pathophysiology of HT and GD, despite their relatively lower abundances, should not be overlooked. The four least abundant genera that differed significantly between thyroid patients and

controls included *Flavonifractor*, *Hungatella*, *Erysipelatoclostridium*, and *Acinetobacter*; all are elevated in other diseases [32–35]. *Bacteroides, Flavonifractor*, *Hungatella*, and *Erysipelatoclostridium* negatively correlated with T3 and T4 levels and positively correlated with TSH levels. Regarding the above results, we speculate that the pathogenic microbiota, at least in part, may synergistically affect thyroid function, requiring advanced research.

Faecalibaterium prausnitzii, the unique identifier specie of the genus *Faecalibaterium*, can inhibit the nuclear factor kappa-B and T helper cell 17/Interleukin-17 pathways to maintain intestinal immune homeostasis [36–38]. Moreover, butyrate produced by *Faecalibaterium* regulates oxidative stress by reducing peroxidase and cyclooxygenase and inhibiting inflammatory cytokine expression, thereby ameliorating inflammation along the intestinal mucosa [39]. Thus, reduced levels of *Faecalibaterium* may be crucial to the pathogenesis of hypothyroidism in certain patients.

Many studies have demonstrated correlations between lipid metabolism and factors, including microbiota and thyroid hormones [40,41]. In our study, the significant metabolites identified were also dominated by lipids and lipid-like molecules. Co-occurrence network analysis revealed that cluster 2, primarily composed of lipids metabolites, were likely to be a pivotal mediator in the interactions between butyrate-producing bacteria and the thyroid [41]. Notably, only cortisone and pantothenic acid, matched in lipid and cofactors and vitamin metabolism, respectively, appear to be the specific mediators communicating between the intestinal microbiota and the thyroid. The flavonoids, including (−)-Epicatechin 3′-*O*-glucuronide, and Epifisetinidol-(4beta->8)-epicatechin-(6->4beta)-epifisetinidol were also significantly elevated in HT patients. According to reports, flavonoids can reduce thyroid hormone synthesis by inhibiting thyroid iodine uptake [42]. It is thus possible that the elevated flavonoid levels observed in the HT patients may have directly contributed to their reduced thyroid hormone levels, leading to hypothyroidism. Moreover, Kaeko Murota et al. discovered that intestinal microbiota is involved in flavonoid metabolism, suggesting that flavonoids may play a communicative role in the interactions between gut microbiota and the thyroid [43]. Therefore, this can reasonably explain why HT patients have a higher abundance of *Flavonifractor*, a kind of microorganism related to the utilization of flavonoids, in their stool samples than GD patients. Notably, gut microbiota and metabolites could be candidate biomarkers for characterizing the gut microecology of our patients, as their AUCs were greater than 0.7; however, the combination of genera and metabolites performed better.

However, some limitations of this study must be addressed in future studies. Large sample populations are still needed to demonstrate whether there are indeed substantial differences in the biomarkers derived from the gut microbiome and metabolites. Metagenomics research will be needed to elucidate the active gut microbiome in thyroid patients more thoroughly. Another limitation of this study is that high-throughput sequencing observed a reduced abundance of butyrate-producing bacteria, but metabolomics studies did not find a corresponding reduction in butyrate. This may be partly due to the low concentration of butyrate, but also due to insufficient targeting of non-target technologies to detect more finely classified metabolites. Therefore, targeted metabolomics could be used in subsequent studies to further investigate the mechanisms regarding the gut-thyroid axis.

5. Conclusions

Briefly, our data reveal the association between gut microbiota and metabolites and thyroid functions from a multi-omics perspective. Combined with studies of other autoimmune diseases, such as Hashimoto and rheumatoid arthritis, this study may provide evidence for a hypothesis that changes in the gut microbiota are related to the pathogenesis of autoimmune diseases [8,44]. It lays a research foundation for microbiota refinement and provides a comprehensive understanding of clinical prevention and a potential noninvasive tool for disease management.

Data availability statement

The raw sequence data has been deposited and available in the National Center for Biotechnology Information database under accession number PRJNA1005070.

Ethics statement

This study was reviewed and approved by the Ethics Committee of Shanghai Tenth People's Hospital, with the approval number: 2020-KN73-01. All participants provided informed consent to participate in the study.

Funding statement

This study was sponsored by National Natural Science Foundation of China [82071964], Shanghai Leading Talent Program [03.05.19005], Shanghai Shenkang Three-year Action Project [SHDC2020CR2054B], Shanghai Municipal Health Commission [GWV-10.1-XK9], and Natural Science Foundation of Shanghai [21ZR1449600].

CRediT authorship contribution statement

Wen Jiang: Data curation, Formal analysis, Investigation, Methodology, Visualization, Writing – original draft. **Ganghua Lu:** Formal analysis, Methodology, Visualization, Writing – original draft. **Tingting Qiao:** Formal analysis, Software, Investigation. **Xiaqing Yu:** Formal analysis, Software, Validation. **Qiong Luo:** Project administration, Resources. **Junyu Tong:** Formal analysis,

Investigation, Software. **Suyun Fan:** Project administration, Resources. **Li Chai:** Project administration, Resources. **Dingwei Gao:** Formal analysis, Software. **Ru Wang:** Formal analysis, Software, Validation. **Chengwen Deng:** Formal analysis, Software, Visualization. **Zhongwei Lv:** Funding acquisition, Project administration, Supervision. **Dan Li:** Funding acquisition, Project administration, Supervision, Writing – review & editing.

Declaration of competing interest

The authors declare that they have no known competing financial interests or personal relationships that could have appeared to influence the work reported in this paper.

Acknowledgements

We thank Home for Researchers editorial team (www.home-for-researchers.com) for language editing service.

Abbreviations

GD: Graves' disease; HT: hypothyroidism; TSH: thyroid stimulating hormone; TRAb: thyroid stimulating hormone receptor antibody; FT4: free thyroxine; BMI: body mass index; FT3: free triiodothyronine; TT3: total triiodothyronine; TT4: total thyroxine; LC-MS: liquid chromatography-mass spectrometry; QC: quality control; OTUs: operational taxonomy units; PLS-DA: partial least squares discriminant analysis; PERMANOVA: permutational multivariate analysis of variance; LDA: linear discriminant analysis; LEfSe: linear discriminant analysis effect size; OPLS-DA: orthogonal projections to latent structures-discriminant analysis; VIP: variable importance in the projection; KEGG: kyoto encyclopedia of genes and genomes; F/B: ratios of *Firmicutes* to *Bacteroidetes*; RF: random forest; ROC: receiver operating characteristic curve; AUC: area under the curve.

Appendix A. Supplementary data

Supplementary data to this article can be found online at https://doi.org/10.1016/j.heliyon.2023.e21463.

References

[1] J.S. Severo, J.B.S. Morais, T.E.C. De Freitas, A.L.P. Andrade, M.M. Feitosa, L.C. Fontenelle, A.R.S. De Oliveira, K.J.C. Cruz, D. Do Nascimento Marreiro, The role of Zinc in thyroid hormones metabolism, Int. J. Vitam. Nutr. Res. 89 (2019) 80–88, https://doi.org/10.1024/0300-9831/a000262.
[2] T. Reinehr, Obesity and thyroid function, Mol. Cell. Endocrinol. 316 (2010) 165–171, https://doi.org/10.1016/j.mce.2009.06.005.
[3] R. Hanoa, R. Hansen, T. Nilsen, A medical information system for the Norwegian continental shelf (MICS), NIPH annals 6 (1983) 17–21.
[4] I. Subekti, L.A. Pramono, Current diagnosis and management of Graves' disease, Acta Med. Indones. 50 (2018) 177–182. https://www.ncbi.nlm.nih.gov/pubmed/29950539.
[5] B. Biondi, D.S. Cooper, Thyroid hormone therapy for hypothyroidism, Endocrine 66 (2019) 18–26, https://doi.org/10.1007/s12020-019-02023-7.
[6] W. Jiang, X. Yu, R.O. Kosik, Y. Song, T. Qiao, J. Tong, S. Liu, S. Fan, Q. Luo, L. Chai, Z. Lv, D. Li, Gut microbiota may play a significant role in the pathogenesis of Graves' disease, Thyroid 31 (2021) 810–820, https://doi.org/10.1089/thy.2020.0193.
[7] C. Virili, P. Fallahi, A. Antonelli, S. Benvenga, M. Centanni, Gut microbiota and Hashimoto's thyroiditis, Rev. Endocr. Metab. Disord. 19 (2018) 293–300, https://doi.org/10.1007/s11154-018-9467-y.
[8] S. Liu, Y. An, B. Cao, R. Sun, J. Ke, D. Zhao, The composition of gut microbiota in patients Bearing Hashimoto's thyroiditis with euthyroidism and hypothyroidism, Internet J. Endocrinol. 2020 (2020), 5036959, https://doi.org/10.1155/2020/5036959.
[9] H. Ishaq, I. Mohammad, M. Shahzad, C. Ma, M. Raza, X. Wu, H. Guo, P. Shi, J. Xu, Molecular alteration analysis of human gut microbial composition in Graves' disease patients, Int. J. Biol. Sci. 14 (2018) 1558–1570, https://doi.org/10.7150/ijbs.24151.
[10] F. Zhao, J. Feng, J. Li, L. Zhao, Y. Liu, H. Chen, Y. Jin, B. Zhu, Y. Wei, Alterations of the gut microbiota in Hashimoto's thyroiditis patients, thyroid, official journal of the American Thyroid Association 28 (2018) 175–186, https://doi.org/10.1089/thy.2017.0395.
[11] F. Sasso, O. Carbonara, R. Torella, A. Mezzogiorno, V. Esposito, L. Demagistris, M. Secondulfo, R. Carratu, D. Iafusco, M. Cartenì, Ultrastructural changes in enterocytes in subjects with Hashimoto's thyroiditis, Gut 53 (2004) 1878–1880, https://doi.org/10.1136/gut.2004.047498.
[12] Q. Mu, J. Kirby, C. Reilly, X. Luo, Leaky gut as a danger signal for autoimmune diseases, Front. Immunol. 8 (2017) 598, https://doi.org/10.3389/fimmu.2017.00598.
[13] D.S. Ross, H.B. Burch, D.S. Cooper, M.C. Greenlee, P. Laurberg, A.L. Maia, S.A. Rivkees, M. Samuels, J.A. Sosa, M.N. Stan, M.A. Walter, American thyroid association guidelines for diagnosis and management of hyperthyroidism and other causes of thyrotoxicosis, Thyroid 26 (2016) (2016) 1343–1421, https://doi.org/10.1089/thy.2016.0229.
[14] N. Segata, J. Izard, L. Waldron, D. Gevers, L. Miropolsky, W.S. Garrett, C. Huttenhower, Metagenomic biomarker discovery and explanation, Genome Biol. 12 (2011) R60, https://doi.org/10.1186/gb-2011-12-6-r60.
[15] R.C. Edgar, B.J. Haas, J.C. Clemente, C. Quince, R. Knight, UCHIME improves sensitivity and speed of chimera detection, Bioinformatics 27 (2011) 2194–2200, https://doi.org/10.1093/bioinformatics/btr381.
[16] J. Navas-Molina, J. Peralta-Sánchez, A. González, P. Mcmurdie, Y. Vázquez-Baeza, Z. Xu, L. Ursell, C. Lauber, H. Zhou, S. Song, J. Huntley, G. Ackermann, D. Berg-Lyons, S. Holmes, J. Caporaso, R. Knight, Advancing our understanding of the human microbiome using QIIME, Methods Enzymol. 531 (2013) 371–444, https://doi.org/10.1016/b978-0-12-407863-5.00019-8.
[17] J. Xia, I. Sinelnikov, B. Han, D. Wishart, MetaboAnalyst 3.0–making metabolomics more meaningful, Nucleic Acids Res. 43 (2015) W251–W257, https://doi.org/10.1093/nar/gkv380.
[18] M.S. Cline, M. Smoot, E. Cerami, A. Kuchinsky, N. Landys, C. Workman, R. Christmas, I. Avila-Campilo, M. Creech, B. Gross, K. Hanspers, R. Isserlin, R. Kelley, S. Killcoyne, S. Lotia, S. Maere, J. Morris, K. Ono, V. Pavlovic, A.R. Pico, A. Vailaya, P.L. Wang, A. Adler, B.R. Conklin, L. Hood, M. Kuiper, C. Sander, I. Schmulevich, B. Schwikowski, G.J. Warner, T. Ideker, G.D. Bader, Integration of biological networks and gene expression data using Cytoscape, Nat. Protoc. 2 (2007) 2366–2382, https://doi.org/10.1038/nprot.2007.324.

[19] A. Schwiertz, D. Taras, K. Schäfer, S. Beijer, N.A. Bos, C. Donus, P.D. Hardt, Microbiota and SCFA in lean and overweight healthy subjects, Obesity 18 (2010) 190–195, https://doi.org/10.1038/oby.2009.167.

[20] J. Feng, F. Zhao, J. Sun, B. Lin, L. Zhao, Y. Liu, Y. Jin, S. Li, A. Li, Y. Wei, Alterations in the gut microbiota and metabolite profiles of thyroid carcinoma patients, Int. J. Cancer 144 (2019) 2728–2745, https://doi.org/10.1002/ijc.32007.

[21] D. Mariat, O. Firmesse, F. Levenez, V. Guimarães, H. Sokol, J. Doré, G. Corthier, J.P. Furet, The Firmicutes/Bacteroidetes ratio of the human microbiota changes with age, BMC Microbiol. 9 (2009) 123, https://doi.org/10.1186/1471-2180-9-123.

[22] A. Koliada, G. Syzenko, V. Moseiko, L. Budovska, K. Puchkov, V. Perederiy, Y. Gavalko, A. Dorofeyev, M. Romanenko, S. Tkach, L. Sineok, O. Lushchak, A. Vaiserman, Association between body mass index and Firmicutes/Bacteroidetes ratio in an adult Ukrainian population, BMC Microbiol. 17 (2017) 120, https://doi.org/10.1186/s12866-017-1027-1.

[23] X. Su, Y. Zhao, Y. Li, S. Ma, Z. Wang, Gut Dysbiosis Is Associated with Primary Hypothyroidism with Interaction on Gut-Thyroid axis, Clinical science, London, England, 2020, pp. 1521–1535, https://doi.org/10.1042/cs20200475, 1979). 134.

[24] G. Kakiyama, W. Pandak, P. Gillevet, P. Hylemon, D. Heuman, K. Daita, H. Takei, A. Muto, H. Nittono, J. Ridlon, M. White, N. Noble, P. Monteith, M. Fuchs, L. Thacker, M. Sikaroodi, J. Bajaj, Modulation of the fecal bile acid profile by gut microbiota in cirrhosis, J. Hepatol. 58 (2013) 949–955, https://doi.org/10.1016/j.jhep.2013.01.003.

[25] F. Van Immerseel, R. Ducatelle, M. De Vos, N. Boon, T. Van De Wiele, K. Verbeke, P. Rutgeerts, B. Sas, P. Louis, H. Flint, Butyric acid-producing anaerobic bacteria as a novel probiotic treatment approach for inflammatory bowel disease, J. Med. Microbiol. 59 (2010) 141–143, https://doi.org/10.1099/jmm.0.017541-0.

[26] S. Gerhardt, M. Mohajeri, Changes of colonic bacterial composition in Parkinson's disease and other neurodegenerative diseases, Nutrients 10 (2018), https://doi.org/10.3390/nu10060708.

[27] V. Smirnov, V. Makhovskiĭ, [Cicatricial stenosis of the stomach and small intestine after a chemical burn], Khirurgiia (1984) 138.

[28] N. Singh, A. Gurav, S. Sivaprakasam, E. Brady, R. Padia, H. Shi, M. Thangaraju, P.D. Prasad, S. Manicassamy, D.H. Munn, J.R. Lee, S. Offermanns, V. Ganapathy, Activation of Gpr109a, receptor for niacin and the commensal metabolite butyrate, suppresses colonic inflammation and carcinogenesis, Immunity 40 (2014) 128–139, https://doi.org/10.1016/j.immuni.2013.12.007.

[29] C. Brown, A. Davis-Richardson, A. Giongo, K. Gano, D. Crabb, N. Mukherjee, G. Casella, J. Drew, J. Ilonen, M. Knip, H. Hyöty, R. Veijola, T. Simell, O. Simell, J. Neu, C. Wasserfall, D. Schatz, M. Atkinson, E. Triplett, Gut microbiome metagenomics analysis suggests a functional model for the development of autoimmunity for type 1 diabetes, PLoS One 6 (2011), e25792, https://doi.org/10.1371/journal.pone.0025792.

[30] Y. Wei, Y. Li, L. Yan, C. Sun, Q. Miao, Q. Wang, X. Xiao, M. Lian, B. Li, Y. Chen, J. Zhang, Y. Li, B. Huang, Y. Li, Q. Cao, Z. Fan, X. Chen, J.Y. Fang, M.E. Gershwin, R. Tang, X. Ma, Alterations of gut microbiome in autoimmune hepatitis, Gut 69 (2020) 569–577, https://doi.org/10.1136/gutjnl-2018-317836.

[31] E. Kiseleva, K. Mikhailopulo, O. Sviridov, G. Novik, Y. Knirel, E. Szwajcer Dey, The role of components of Bifidobacterium and Lactobacillus in pathogenesis and serologic diagnosis of autoimmune thyroid diseases, Benef. Microbes 2 (2011) 139–154, https://doi.org/10.3920/bm2010.0011.

[32] A. Genoni, C. Christophersen, J. Lo, M. Coghlan, M. Boyce, A. Bird, P. Lyons-Wall, A. Devine, Long-term Paleolithic diet is associated with lower resistant starch intake, different gut microbiota composition and increased serum TMAO concentrations, Eur. J. Nutr. 59 (2020) 1845–1858, https://doi.org/10.1007/s00394-019-02036-y.

[33] F.K. Berger, N. Schwab, M. Glanemann, R.M. Bohle, B. Gärtner, H.V. Groesdonk, Flavonifractor (Eubacterium) plautii bloodstream infection following acute cholecystitis, IDCases 14 (2018), e00461, https://doi.org/10.1016/j.idcr.2018.e00461.

[34] T. Shao, L. Shao, H. Li, Z. Xie, Z. He, C. Wen, Combined signature of the fecal microbiome and metabolome in patients with gout, Front. Microbiol. 8 (2017) 268, https://doi.org/10.3389/fmicb.2017.00268.

[35] I. Chebotar, A. Lazareva, Y. Masalov, V. Mikhailovich, N. Mayanskiy, [Acinetobacter: Microbiological, Pathogenetic and Resistant Properties], Vestnik Rossiiskoi akademii meditsinskikh nauk, 2014, pp. 39–50, https://doi.org/10.15690/vramn.v69i9-10.1130.

[36] F. De Filippis, E. Pasolli, D. Ercolini, Newly explored Faecalibacterium diversity is connected to age, lifestyle, geography, and disease, Curr. Biol. 30 (2020) 4932–4943.e4, https://doi.org/10.1016/j.cub.2020.09.063.

[37] E. Quévrain, M.A. Maubert, C. Michon, F. Chain, R. Marquant, J. Tailhades, S. Miquel, L. Carlier, L.G. Bermúdez-Humarán, B. Pigneur, O. Lequin, P. Kharrat, G. Thomas, D. Rainteau, C. Aubry, N. Breyner, C. Afonso, S. Lavielle, J.P. Grill, G. Chassaing, J.M. Chatel, G. Trugnan, R. Xavier, P. Langella, H. Sokol, P. Seksik, Identification of an anti-inflammatory protein from Faecalibacterium prausnitzii, a commensal bacterium deficient in Crohn's disease, Gut 65 (2016) 415–425, https://doi.org/10.1136/gutjnl-2014-307649.

[38] M. Zhang, X. Qiu, H. Zhang, X. Yang, N. Hong, Y. Yang, H. Chen, C. Yu, Faecalibacterium prausnitzii inhibits interleukin-17 to ameliorate colorectal colitis in rats, PLoS One 9 (2014), e109146, https://doi.org/10.1371/journal.pone.0109146.

[39] H.M. Hamer, D.M. Jonkers, S.A. Vanhoutvin, F.J. Troost, G. Rijkers, A. De Bruïne, A. Bast, K. Venema, R.J. Brummer, Effect of butyrate enemas on inflammation and antioxidant status in the colonic mucosa of patients with ulcerative colitis in remission, Clin Nutr 29 (2010) 738–744, https://doi.org/10.1016/j.clnu.2010.04.002.

[40] Z. Wang, D. Koonen, M. Hofker, J. Fu, Gut microbiome and lipid metabolism: from associations to mechanisms, Curr. Opin. Lipidol. 27 (2016) 216–224, https://doi.org/10.1097/mol.0000000000000308.

[41] A. Delitala, G. Fanciulli, M. Maioli, G. Delitala, Subclinical hypothyroidism, lipid metabolism and cardiovascular disease, Eur. J. Intern. Med. 38 (2017) 17–24, https://doi.org/10.1016/j.ejim.2016.12.015.

[42] C. Gonçalves, M. De Freitas, A. Ferreira, Flavonoids, thyroid iodide uptake and thyroid cancer-A review, Int. J. Mol. Sci. 18 (2017), https://doi.org/10.3390/ijms18061247.

[43] K. Murota, Y. Nakamura, M. Uehara, Flavonoid metabolism: the interaction of metabolites and gut microbiota, Biosci. Biotechnol. Biochem. 82 (2018) 600–610, https://doi.org/10.1080/09168451.2018.1444467.

[44] Y. Sun, Q. Chen, P. Lin, R. Xu, D. He, W. Ji, Y. Bian, Y. Shen, Q. Li, C. Liu, K. Dong, Y.W. Tang, Z. Pei, L. Yang, H. Lu, X. Guo, L. Xiao, Characteristics of gut microbiota in patients with rheumatoid arthritis in Shanghai, China, Front. Cell. Infect. Microbiol. 9 (2019) 369, https://doi.org/10.3389/fcimb.2019.00369.